

DOI:10.1002/ejic.201201050

Donor Abilities of Heterocyclic Neutral Lewis Bases in a Nickel(II) Salicylaldehyde 4-Phenylthiosemicarbazonato Coordination Environment

Marina Cindrić,^{*,[a]} Gordana Pavlović,^{*,[b]} Tomica Hrenar,^[a]
Marina Uzelac,^[a] and Manda Ćurić^[c]

Keywords: Nickel / S,N ligands / Lewis bases / Hydrogen bonds

Eight mononuclear [Ni(sal4-Phtsc)-D] thiosemicarbazonato complexes [sal4-Phtsc = salicylaldehyde 4-phenylthiosemicarbazonato ligand; D = imidazole (1), methylimidazole (2), pyridine (3), 4-aminopyridine (4), 4-methylpyridine (6), morpholine (7), thiomorpholine (8), 2-aminophenol (9)] and one dinuclear [(Ni(sal4-Phtsc))₂·D]·2DMSO [D = 4,4'-bipyridine (5)] complex have been prepared by adding the corresponding Lewis base to the methanol suspension of the parent complex [Ni(sal4-Phtsc)(H₂sal4-Phtsc)]·CH₃OH. The exchange of the neutral salicylaldehyde 4-phenylthiosemicarbazone (H₂sal4-Phtsc) ligand in the parent complex for the appropriate Lewis base has been confirmed by IR spectroscopy and powder X-ray diffraction (PXRD) in the solid state. The single-crystal X-ray diffraction of seven complexes 1 and 3–8 confirmed the formation of the complexes with the

Ni^{II} ion, coordinated through O,N,S-donor atoms from the dibasic salicylaldehyde 4-phenylthiosemicarbazonato ligand and endocyclic N-donor atom from the neutral ligand D in the form of a distorted square-planar coordination. NMR spectroscopy in DMF or DMSO and quantum mechanical calculations have been performed in order to explain and compare the stability of the complexes in solution, depending on the polarity of solvents in the context of donor properties and the nucleophilicity of the heterocyclic Lewis base. The single-crystal X-ray data enables a comparison with calculated standard Gibbs energies of binding in the context of crystal packing forces, leading to a general conclusion that the stability of the mononuclear complexes results in the formation of more stable hydrogen-bonded cyclic dimers as a crystal packing pattern.

Introduction

Nickel is an essential trace element for living organisms and nickel enzymes known to date are divided into two groups: hydrolases and redox enzymes. Nickel(II) acts as the Lewis acid in hydrolase enzymes, while the presence of SH coordination of redox active enzymes is crucial for catalytic cycles of nickel centres.^[1–4] Although the discovery of urease as the first biological system for which nickel is essential for activity dates to 1975 and despite several thorough studies on biochemical and physical properties of nickel enzymes, we do not have all the answers as to how

the different ligands enhance the catalysis of all the reactions. In recent years investigations have been done on structural and biological properties of thiosemicarbazones and their complexes as a potential model system for redox enzymes.^[2–8] Thiosemicarbazones have received considerable attention because of their coordination chemistry^[9–11] and biological activities. Thiosemicarbazones derived from 2-hydroxy-aromatic aldehydes such as H₂sal4-Phtsc can ligate metal centres in a monodentate or chelate mode through a S-donor atom or O,N,S-donor system. While free tsc ligands are dominated by the thione tautomeric form, both thione and thiol tautomers can be presented in metal complexes, sometimes in the same complex. Thiosemicarbazones derived from 2-hydroxy-aromatic aldehydes, which coordinate metal ions monodentately or tridentately, are in the thione and thiol form, respectively. Dibasic forms of such tridentate ligands are generated by the deprotonation of –OH and –SH groups.

Their biological properties and activities are often related to their ability to form chelates with metal ions and to the presence of a substituent at the peripheral nitrogen atom.^[4] Minor modifications in thiosemicarbazonato ligands, such as the bulky substituent at the peripheral nitrogen atom, can cause substantial changes in their biological and pharmacological properties.^[12] The biological activity of thio-

[a] Faculty of Science, University of Zagreb, Horvatovac 102a, Zagreb 10000, Croatia
Fax: +385-1-461-1191
E-mail: marina@chem.pmf.hr
Homepage: www.chem.pmf.hr

[b] Faculty of Textile Technology, Department of Applied Chemistry, University of Zagreb, Prilaz baruna Filipovića 28a, Zagreb 10000, Croatia
Fax: +385-1-3712-599
E-mail: gpavlov2@ttf.hr
Homepage: www.unizg.ttf.hr

[c] Rudjer Bošković Institute, P. O. Box 1016, Zagreb 10000, Croatia
Homepage: www.irb.hr

Supporting information for this article is available on the WWW under <http://dx.doi.org/10.1002/ejic.201201050>.

semicarbazonato complexes differs from that of either of the ligands or the metal ions and is increased and/or decreased, depending on lipophilicity, which controls the rate of entry of molecules or ions into the cell, and is modified by coordination.^[5] This is a very important process that modulates electronic properties and activity of the metal centre and is decisive for the activity of metalloenzymes, because it changes the coordination around the metal centre by breaking and forming coordinative bonds with substrates or other molecules.

Because of their promising biological and catalytic activities, salicylaldehyde thiosemicarbazonato nickel(II) complexes with different substituents at the peripheral N³ atom have been studied extensively.^[13–15] Recently, we have investigated new synthetic routes, such as mechanochemical and electrochemical ones, in the preparation of square-planar and octahedral nickel(II) complexes with salicylaldehyde thiosemicarbazone ligands. The ligands were substituted at the peripheral N³ atom. We have compared these non-conventional routes with the classical approach.^[16] We have also studied the influence of synthetic conditions on the coordination around Ni^{II}, since the control of geometry and spin states of metal ions has a very important role in inorganic and biological chemistry, especially in catalytic processes. In a continuation of the investigations of salicylaldehyde thiosemicarbazonato Ni^{II} complexes we have prepared eight mononuclear complexes and one dinuclear of the type [Ni(sal4-Phtsc)·D] and {[Ni(sal4-Phtsc)]₂·D}·2DMSO. Square-planar Ni^{II} complexes are coordinated with the tridentate salicylaldehyde 4-phenylthiosemicarbazonato ligand, while the fourth coordination site is occupied by a heterocyclic Lewis base, D [D = imidazole (1), methylimidazole (2), pyridine (3), 4-aminopyridine (4), 4,4'-bipyridine (5), 4-methylpyridine (6), morpholine (7), thiomorpholine (8) and 2-aminophenol (9)]; see Figure 1, parts a–c, the complexes 1 and 5 are chosen as representatives.

The complexes were characterized by NMR spectroscopy in solution and IR spectroscopy, powder X-ray diffraction (PXRD) and single-crystal X-ray diffraction (SCXRD) in the solid state, in order to follow up the donor abilities of various Lewis bases in a salicylaldehyde 4-phenylthiosemicarbazonato environment of Ni^{II} complexes, i.e. the competition of provided donor atoms for the Ni^{II} coordination sphere. The X-ray structural analysis of the majority of the prepared complexes (1 and 3–8) enables us to follow the placement of the Lewis base molecule in the coordination sphere of the Ni^{II} ion and its influence on the conformation and stability of the complex molecule in the solid state. These effects are accompanied by quantum mechanical calculations of standard Gibbs energies of binding in vacuo and in the solvents of differing polarity.

Results and Discussion

General Considerations

During our investigations on the synthesis and characterization of the thiosemicarbazonato Ni^{II} complexes,^[16] we

observed the decomposition of the [Ni(sal4-Phtsc)(H₂sal4-Phtsc)]·CH₃OH complex in the DMSO solution and the substitution of the S-bound H₂sal4-Phtsc ligand by a DMSO molecule. This reaction inspired us to investigate the influence of various neutral Lewis bases on the nickel(II) coordination sphere, according to their nucleophilicity and stereochemistry. A number of square-planar Ni^{II} salicylaldehyde 4-phenylthiosemicarbazonato complexes are known where monodentate ligands with N- or P-donor atoms occupy the fourth coordination site, but a study on the influence of the nucleophilicity and stereochemistry of ligands providing N, O/N or N/S donor sets is absent.^[17] The reactions of [Ni(sal4-Phtsc)(H₂sal4-Phtsc)]·CH₃OH with different Lewis bases such as imidazole (1), 2-methylimidazole (2), pyridine (3), 4-aminopyridine (4), 4,4'-bipyridine (5), 4-methylpyridine (6), morpholine (7), thiomorpholine (8) and 2-aminophenol (9) yielded new crystalline square-planar Ni^{II} complexes. (Figure 1). All the complexes are red to orange in colour and soluble in most organic solvents. Superimposition of the experimental powder patterns confirms the structural differences for complexes 1–9 mutually and in relation to the parent complex (Figure S2).

IR Spectroscopy

Their IR spectra are in accordance with the literature data for similar types of compounds (Figure S1).^[18] In all complexes, the bands observed over the range 3349 to 3127 cm⁻¹ correspond to ν(O–H) and ν(N–H) stretching vibrations from the thiosemicarbazonato ligand. The strong ν(C=N) bands between 1606 and 1581 cm⁻¹ indicate the coordination of the azomethine nitrogen to Ni^{II}. The thioamide bands, ν(C–S), lie in the range 820–860 cm⁻¹, and indicate the coordination of Ni^{II} to the sulfur atom. The ligation of the Lewis bases, morpholine, 2-aminophenol and thiomorpholine, takes place through a N-donor atom, and the characteristic C–N bands appear in the spectra of 7, 8 and 9 at 1112, 1114 and 1212 cm⁻¹.

Crystal Structure Description

The molecular structures of the six mononuclear complexes, [Ni(sal4-Phtsc)·D] (1, 3, 4 and 6–8) and one dinuclear complex, {[Ni(sal4-Phtsc)]₂·D}·2DMSO (5), were determined by single-crystal X-ray diffraction studies (Figure 1 and Supporting Information, Figures S3–S7). Complex 3 is the conformational polymorph of the previously published pyridine derivative,^[13k] which contains two conformers of complex molecules within an asymmetric unit. A comparison of the powder patterns calculated from the single-crystal data along with overlaying of molecular structures confirms conformational differences between 3 and the previously published polymorph (Figure S8 and S9, respectively). The asymmetric unit of each molecular structure contains one complex molecule, except in the case of structure 8 with two crystallographically independent molecules per asymmetric unit. The two complex molecules dif-

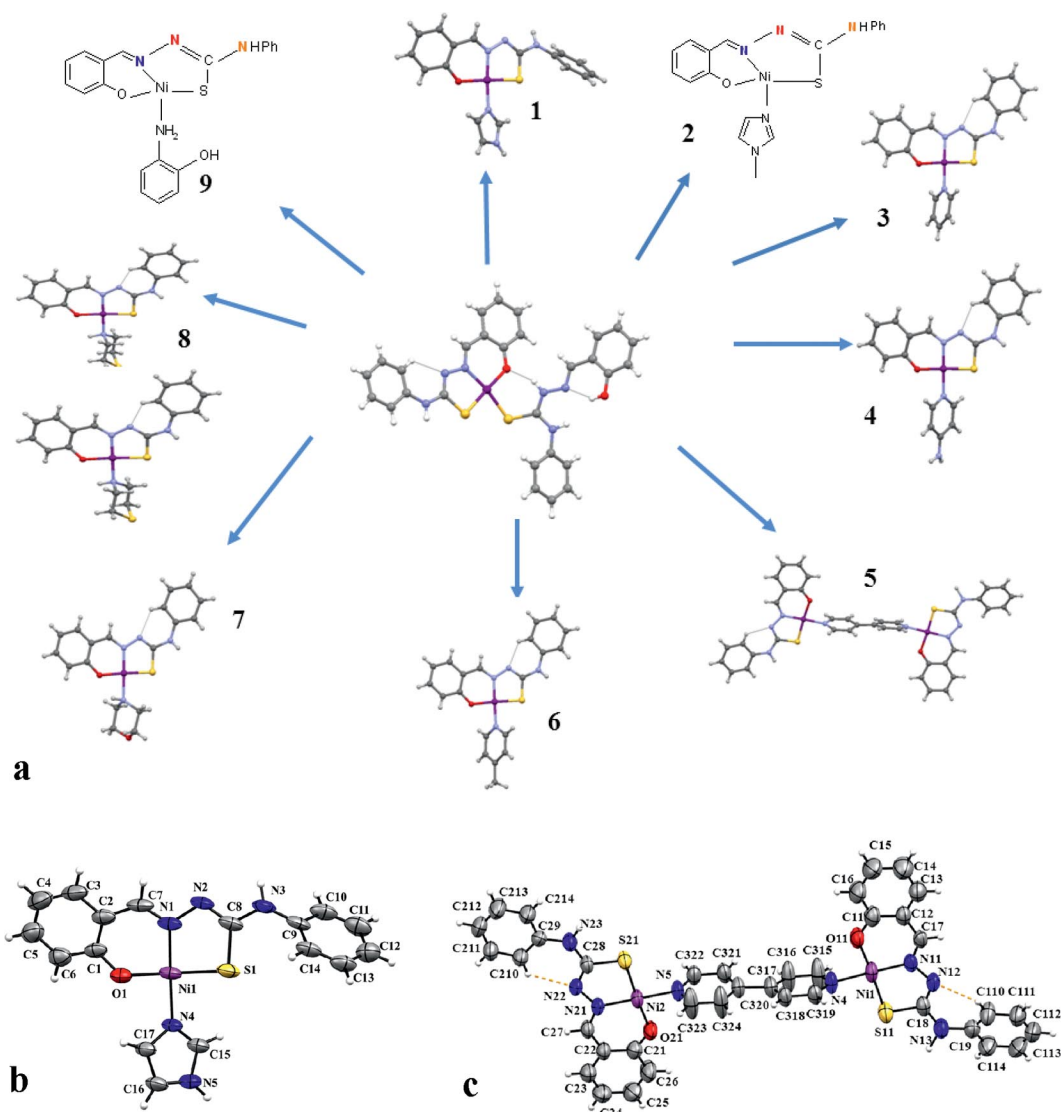


Figure 1. (a) Schematic overview of complexes **1–9** obtained from the reaction of complex $[\text{Ni}(\text{sal4-Phtsc})(\text{H}_2\text{sal4-Phtsc})]\cdot\text{CH}_3\text{OH}$ with the methanol suspension of the corresponding Lewis base. The Mercury rendered view of the ball and stick molecular structures of complexes **1** and **3–8** are shown. The colour scheme applied is: Ni – purple, S – yellow, oxygen – red, nitrogen – blue, carbon – gray, hydrogen – light gray. The almost identical molecular orientations can be seen. The dashed lines represent weak intramolecular C14–H14–N2 hydrogen bonds in complexes **3–8**. The probable structures of complexes **2** and **9** are outlined by chemical diagrams. Solvent DMSO molecules in **5** are omitted. The asymmetric unit of complex **8** with two crystallographically independent complex molecules is shown. (b) The Mercury POV-Ray view of the asymmetric unit of **1** with the atom-labelling scheme. The displacement ellipsoids are drawn at the 50% probability level at 296(2) K. (c) The Mercury POV-Ray view of the asymmetric unit of **5** with the atom-labelling scheme. The displacement ellipsoids are drawn at the 50% probability level at 296(2) K. DMSO molecules are omitted.

fer mainly in the *N*-phenyl ring conformation (Figure S10). The crystal structure of complex **5** contains two DMSO molecules as the solvent of crystallization. The Ni^{II} ion is chelated in a square-planar deformed coordination by the sal4-Phtsc tridentate dibasic ligand through the thioamide sulfur, azomethine nitrogen and phenolato oxygen atoms and by the nitrogen atom from the heterocyclic neutral Lewis base *trans* to the azomethine nitrogen atom (Table 1). Such chelation results in the formation of two chelate rings: six-membered and five-membered ring with the azomethine nitrogen atom acting as a common atom, forming a bicyclic system slightly folded along the nickel-to-imine nitrogen axis.

The nickel to sulfur bond lengths (which are always shorter for the thiol form than that of the thione due to the chelate effect, since the chelate rings have a pseudoaromatic character)^[13] indicate a $-\text{C}=\text{N}=\text{C}-\text{SH}$ thiol form of the sal4-Phtsc ligand along with the other bond lengths of the central ligand backbone, such as the nitrogen-to-carbon bond length in the $-\text{N}=\text{C}-\text{SH}$ region, which has a significant π character, and the carbon-to-sulfur bond length, which is dominantly σ in character.

The sal4-Phtsc ligand consists of three structural fragments: the salicyl part, the central thiosemicarbazonyl moiety and the phenyl part. The salicyl-thiosemicarbazonyl moiety is almost planar, while the lack of planarity of the

Table 1. Nickel(II) coordination sphere geometry (bond lengths [Å] and angles [°]) for the **1** and **3–8** complexes. *The corresponding values in **5** and **8** are: Ni1–S11, Ni1–O11, Ni1–N11, Ni1–N14, Ni2–S21, Ni2–O21, Ni2–N21 and Ni2–N24. **D: nitrogen atom from the neutral Lewis base.

	1	3	4	5*	6	7	8*
Bond lengths							
Ni1–S1	2.138(1)	2.153(2)	2.156(1)	2.140(3) 2.140(2)	2.1586(7)	2.151(4)	2.143(2) 2.144(1)
Ni1–O1	1.862(2)	1.873(5)	1.879(2)	1.856(6) 1.856(5)	1.862(2)	1.843(8)	1.858(3) 1.851(3)
Ni1–N1	1.851(3)	1.862(6)	1.852(2)	1.858(5) 1.854(5)	1.854(2)	1.856(9)	1.871(4) 1.862(4)
Ni1–D**	1.911(2)	1.928(5)	1.908(2)	1.925(5) 1.920(5)	1.914(2)	1.953(8)	1.960(4) 1.958(4)
Bond angles							
N1–Ni1–O1	94.8(1)	95.4(2)	95.29(7)	95.4(3) 95.6(2)	95.61(8)	95.3(4)	95.3(2) 95.3(2)
N1–Ni1–D	174.3(1)	177.4(3)	175.92(8)	178.2(3) 177.3(3)	177.83(8)	178.0(4)	179.2(2) 179.5(2)
O1–Ni1–D	87.8(1)	86.4(2)	86.88(7)	86.4(3) 86.1(2)	86.00(7)	84.0(4)	84.5(2) 84.5(2)
N1–Ni1–S1	87.1(1)	87.4(2)	87.15(6)	87.8(2) 87.6(2)	87.09(6)	87.1(4)	87.1(1) 87.2(1)
O1–Ni1–S1	172.6(1)	176.5(2)	176.05(5)	176.8(2) 175.9(2)	176.95(5)	177.0(3)	177.3(1) 177.5(1)
D–Ni1–S1	91.1(1)	90.9(2)	90.87(5)	90.4(2) 90.8(2)	91.34(6)	93.6(3)	93.2(1) 93.1(1)

ligand as a whole is described by dihedral angles calculated between the two peripheral phenyl rings of the sal4-Phtsc ligand in **1** and **3–8** (Table S4). The significant discrepancy in the dihedral angle value among all complexes is observed only for structure **1** [Table S4; 80.6(2)°]. The configuration of the sal4-Phtsc ligand reveals that the sulfur atom is oriented at the same side as the –NH group in the complexes **3–8**, but not in the imidazole derivative **1**. This is evidenced by the twisting of the phenyl ring in the –NHPh moiety around the C8–N3 single bond *trans* to the sulfur atom (Figure 2 and Table S5). Many structures of uncomplexed and unprotonated thiosemicarbazones reveal the *trans* configuration of the sulfur atom to the azomethine nitrogen and the *cis* configuration of the –NH group and azomethine nitrogen atom.^[19]

The complexation of the sal4-Phtsc ligand requires a *cis* configuration of the sulfur atom to the azomethine nitrogen, which is afforded in complexes **1** and **3–8**, but not the unavoidable *cis* configuration of the –NH group and azomethine nitrogen atom. The latter configuration of sal4-Phtsc ligand is achieved in complexes **3–8**, while the *trans* configuration of the –NH group and azomethine nitrogen atom is achieved in the imidazole derivative **1**.

The formation of the intramolecular C14–H14...N2 hydrogen bond found in other complexes, is precluded in **1** (Figure 3, a). Both *cis* and *trans* ligand configurations of the –NH and azomethine nitrogen atom can be stabilized by different intermolecular hydrogen bonds, consequently accomplishing similar crystal architectures of the complexes (Figure 3). The sal4-Phtsc ligand configuration in **1** is assisted by the formation of the N–H...N type of intermolecular hydrogen bond between the –NH and azomethine

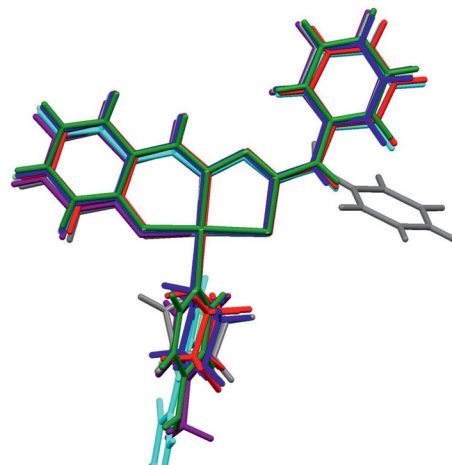


Figure 2. The Mercury rendered view of the overlapping diagram for compounds **1** and **3–8**. The applied colour scheme is: gray – **1**, yellow – **3**, green – **4**, cyan – **5**, purple – **6**, blue – **7** and red – **8** (molecule **1**). The diagrams were constructed by overlapping the molecules through nickel and donor atoms O,N,S. The main conformational misalignment is perceived in the spatial orientation of the Lewis base heterocyclic rings in relation to the salicyl thiosemicarbazone moiety and in the different orientation of the phenyl ring in the –NHPh moiety in the imidazole derivative **1** (in gray) compared with the other structures **3–8** (Table S5).

N1 nitrogen atoms; see Table S3 and part a in Figure 3. In complexes **3**, **4** and **6** the –NH group participates in the N–H...S intermolecular hydrogen-bond formation (Figure 3, b–d). Therefore, the crystal packing patterns are basically characterized by the formation of the centrosymmetric R22(8) rings (in a “carboxylic acid manner”) through either the weak N–H...N intermolecular hydrogen bond in **1** (Fig-

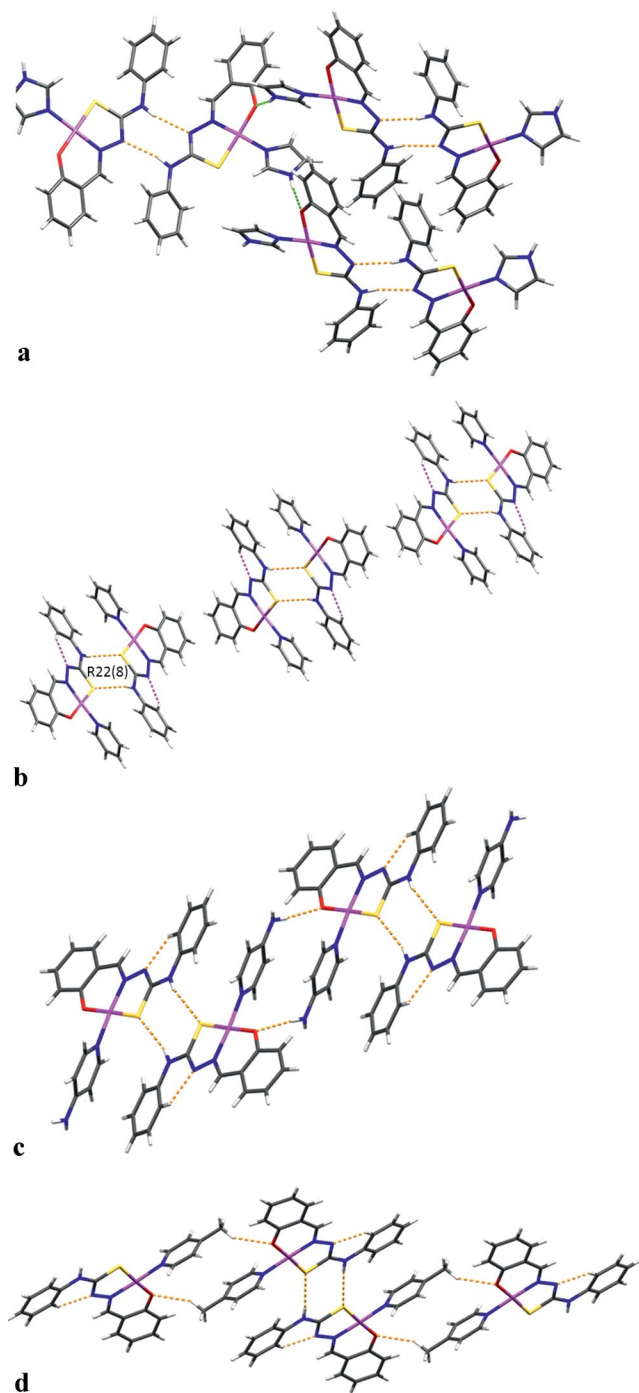


Figure 3. The Mercury POV-Ray rendered view of the different assembly architectures found in the crystal structures of **1**(a), **3**(b), **4**(c) and **6**(d) as a result of the presence of different potential proton donors. The hydrogen bonds are denoted by dashed lines in orange and green. All four packing patterns are basically characterized by the formation of the centrosymmetric R22(8) rings by means of weak N–H...N (in **1**) and N–H...S (**3**, **4** and **6**) intermolecular hydrogen bonds between the N3 atom of the –NHPh moiety and the donor S1 atom. In the crystal structures of **4** and **6** [3(c) and 3(d), respectively] the R22(16) rings are formed by the N–H...O(metal bound) (**4**) or C–H...O(metal bound) (**6**) hydrogen bonds, while in **1** the R22(8) rings are further linked by N(imidazole)–H...O(metal bound) hydrogen bonds (in green) and in **3** by the $\pi\cdots\pi$ interactions (see Supporting Information for further crystal structure descriptions).

ure **3**, a) or the N–H...S intermolecular hydrogen bond in complexes **3**, **4** and **6**, see parts b–d in Figure 3. The cyclic dimers in **1** are further propagated through the N–H...O hydrogen bonds with the imidazole –NH group as a bridge into the 3D hydrogen-bonded network (Figure 3, a). The rings in **3** are stacked along the *b* axis through $\pi\cdots\pi$ interactions. Such molecular piles are arranged in a herringbone fashion along the *c* axis [Table S3 and Figure S11(a)]. On the contrary, hydrogen-bonded dimers in **4** and **6** are additionally connected through N–H...O (in **4**) or C–H...O (in **6**) hydrogen bonds as the result of the presence of NH₂ or CH₃ groups on the pyridine ring at position 4 in complexes **4** and **6**, respectively. Therefore, the new centrosymmetric ring assigned by a graph-set analysis as R22(16) forms a chain of rings alternating with R22(8) rings in **4** and **6** (Figure 3, b–d). The hydrogen-bonded chains are spread along the *a* axis in **4** and **6**. The chains are assembled in a herringbone fashion along the *c* axis; see Table S3 and Figure S11(b) and S11(c). The presence of two DMSO molecules per complex molecule in **5** and acceptor capabilities of the oxygen atom in morpholine (**7**) or the sulfur atom in thiomorpholine (**8**) derivatives prevents the cyclic dimerization found in complexes **1**, **3**, **4** and **6** and enables other crystal packing patterns achieved by the –NH group of the –NHPh structural fragment as a proton donor (Figures S12, S13 and S14).

Theoretical Calculations and Correlation with NMR Spectroscopy

The calculated standard Gibbs energies of binding are in accordance with the experimentally observed trends and linear correlation model between the experimentally measured distances and the calculated standard Gibbs energies of binding for all ligands presented in Table 2 (except for bipyridine). They give an R^2 value of 0.97, confirming the validity of the theoretical methods.

Table 2. The calculated standard Gibbs energies of binding at 298.15 K and 101.325 kPa for complexes of Ni²⁺ with salicylaldehyde 4-phenylthiosemicarbazone and various Lewis bases with the binding atom indicated in parenthesis where necessary. The B3LYP/6-311++g(d,p) level of theory; solvent effects were incorporated using the IEFPCM method.

Complex	$\Delta_r G^\circ_{\text{binding}}$ [kcal mol ⁻¹]			
	in vacuo	in CH ₃ OH ($\epsilon = 32.613$)	in DMF ($\epsilon = 37.219$)	in DMSO ($\epsilon = 46.826$)
1	–612.16	–171.28	–169.43	–167.89
2 (N)	–606.96	–165.69	–163.86	–161.29
3	–609.49	–169.61	–167.83	–165.33
4	–614.58	–173.05	–171.50	–168.60
6	–611.53	–168.90	–167.09	–164.51
7 (N)	–604.55	–165.70	–163.92	–161.41
morpholine (O)	–598.10	–158.81	–157.01	–154.47
8 (N)	–604.11	–165.62	–163.83	–161.34
thiomorpholine (S)	–602.19	–161.92	–160.12	–157.57
dmf (O)	–607.14	–163.45	–161.64	–159.11
dmsO (O)	–607.86	–163.83	–162.01	–159.44

¹H NMR spectroscopic study of complexes **1–9** in [D₆]–DMSO (or [D₇]DMF) solution showed that the structures

of complexes **1**, **5**, **7** and **8** in the solution are consistent with those observed in the solid state (Table S1). The parent complex $[\text{Ni}(\text{sal}4\text{-Phtsc})(\text{H}_2\text{sal}4\text{-Phtsc})]\cdot\text{CH}_3\text{OH}$ and its derivatives **2**, **3**, **4** and **6** decompose very fast in $[\text{D}_6]\text{DMSO}$ producing the $[\text{Ni}(\text{sal}4\text{-Phtsc})(\text{DMSO})]$ complex and a free ancillary ligand, since DMSO replaces S-bound neutral salicylaldehyde 4-phenylthiosemicarbazone in the parent complex, 2-methylimidazole in **2**, pyridine in **3**, 4-aminopyridine in **4** and 4-methylpyridine in **6**.

In contrast to these ligands, imidazole in **1**, 4,4'-bipyridine in **5**, morpholine in **7** and thiomorpholine in **8**, which also act as monodentate ligands (bridging in the case of 4,4'-bipyridine), are more nucleophilic than DMSO and cannot be replaced. Among all the theoretical investigations of the $[\text{Ni}(\text{sal}4\text{-Phtsc})(\text{H}_2\text{sal}4\text{-Phtsc})]\cdot\text{CH}_3\text{OH}$, $[\text{Ni}(\text{sal}4\text{-Phtsc})\text{D}]$ and $\{[\text{Ni}(\text{sal}4\text{-Phtsc})]_2\text{D}\}\cdot 2\text{DMSO}$ complexes with different N-donor Lewis bases, the inclusion of 4-aminopyridine in **4** and imidazole in **1** produced the most stable complexes with the lowest standard Gibbs energies of binding. For complexes **3** and **6**, with pyridine and 4-methylpyridine, respectively, standard Gibbs energies of binding were similar, whereas the introduction of the amino group in the position 4 of the pyridine molecule (in complex **4**) resulted in the significant stabilization of the complex (ca. 4 kcal mol^{-1}). Spectroscopic investigation showed a very fast decomposition of **4** in $[\text{D}_6]\text{DMSO}$ yielding a $[\text{Ni}(\text{sal}4\text{-Phtsc})(\text{DMSO})]$ complex. This is in agreement with the literature data on the influence of nucleophilicity on the complex stability. The oxygen centre in DMSO acts as a nucleophile toward the hard electrophile, such as Ni^{II} , that prefers the oxygen donor site, whereas the nitrogen atom in 4-aminopyridine acts as a soft nucleophile.^[20] The interchange of 4-aminopyridine with DMSO is mostly controlled by the kinetics.^[21] These facts could explain the observation from the temperature-dependent NMR spectra that does not follow the trend in the calculated standard Gibbs energies where complex **4** with the 4-aminopyridine derivative appears to be thermodynamically more stable. In the complexes **7** and **8**, morpholine and thiomorpholine, respectively, are bound to nickel through nitrogen rather than through oxygen or sulfur, as confirmed by single-crystal X-ray diffraction studies. The calculated standard Gibbs energies of the binding of **8** (with thiomorpholine) through a nitrogen or sulfur atom are similar (Table 2). Since this difference is relatively small (ca. 1.9 kcal mol^{-1} in vacuo, giving a 96:4 ratio) both binding modes can be observed, whereas for **8** (with morpholine) this difference is more pronounced ca. 6.4 kcal mol^{-1} in vacuo) favouring only one mode of binding (O over the N atom).

Coordination of the metal atom by nitrogen in these complexes causes a downfield shift of the NH signal by 1.2 and 0.90 ppm, respectively, relative to the signals of free ligands (Scheme S1). In the spectra of the free ligands, morpholine and thiomorpholine, the rings show two resolved triplets resulting from the fast conformational changes. However, these protons in the spectra of the complexes show three or four broad signals at ambient temperature with intensity ratios of 4:2:2 or 2:2:2:2, respectively,

thus demonstrating that the morpholine and thiomorpholine are not locked rigidly into the chair conformation in solution as in the solid state and that their conformation changes are not fast on the NMR timescale. This is supported by variable-temperature ^1H NMR experiments in $[\text{D}_6]\text{DMSO}$ (and $[\text{D}_7]\text{DMF}$) since the spectra recorded in $[\text{D}_6]\text{DMSO}$ at $90\text{ }^\circ\text{C}$ contain only two broad signals. One is the signal of proton H-7, which interacts with oxygen of the six-membered chelate ring.^[22] The other signals of the thiosemicarbazone ligand in the spectrum of complex **9** recorded in $[\text{D}_6]\text{DMSO}$ (or $[\text{D}_7]\text{DMF}$) at ambient temperature are sharp and their integration is in good agreement with the number of protons (Figure S15). However, the signals corresponding to the 2-aminophenol are rather broad and their integration is in disagreement with the number of protons, thus indicating that the $[\text{D}_6]\text{DMSO}$ (or $[\text{D}_7]\text{DMF}$) molecule replacement is fast on the NMR timescale with the 2-aminophenol bound to Ni^{II} in complex **9** through nitrogen of the amino group as suggested by quantum chemical calculations. Similar values for Gibbs energies (Table 2) of binding for complex **9** and DMSO (or DMF) suggested the possibility of ligand interchange with the solvent molecule, which is observable from the low temperature NMR spectra (Figure S15). Hence, in a $[\text{D}_6]\text{DMSO}$ or $[\text{D}_7]\text{DMF}$ solution of complex **9** we assumed a coexistence of complex **9**, complex $[\text{Ni}(\text{sal}4\text{-Phtsc})(\text{DMSO})]$ or $[\text{Ni}(\text{sal}4\text{-Phtsc})(\text{DMF})]$ and free 2-aminophenol, which is supported by variable-temperature ^1H NMR experiments in $[\text{D}_7]\text{DMF}$ (Figure S15). The spectra recorded in $[\text{D}_7]\text{DMF}$ at -25 and $-50\text{ }^\circ\text{C}$ contain very well resolved signals of the 2-aminophenol ligand as well as a H-7 signal of thiosemicarbazone, whose integration is in good agreement with the number of protons, thus demonstrating that in $[\text{D}_7]\text{DMF}$ at -25 and $-50\text{ }^\circ\text{C}$ complex **9** is predominant, since at low temperatures the exchange between solvent molecules and 2-aminophenol is much slower. The coordination of the Ni^{II} by nitrogen of 2-aminophenol in complex **9** results in large downfield shifted signals of NH_2 and OH protons relative to the free ligand signals (Table S1 and Figure S15). A large downfield shift of the OH signal could be a consequence of an intramolecular hydrogen bond between this proton and oxygen of the six-membered chelate ring.^[22] Finally, the calculated Gibbs energies revealed that the stability of all complexes is lower with the increase of the solvent dielectric constant (Table 2).

Conclusions

The square-planar $[\text{Ni}(\text{sal}4\text{-Phtsc})(\text{H}_2\text{sal}4\text{-Phtsc})]\cdot\text{CH}_3\text{OH}$ complex^[16] served as the parent complex in our study on the influence of heterocyclic Lewis bases as monodentate ligands (or bridging in the case of complex **5**) to the nickel(II) coordination sphere, depending on their nucleophilicity and stereochemistry. Our previous investigations on the above-mentioned complex confirmed the labile bonding of the neutral salicylaldehyde 4-phenylthiosemicarbazone ligand to the Ni^{II} ion through a S-donor atom and provided an opportunity to substitute it easily

with different Lewis bases with another –N, –N/O or –N/S donor set introduced by using various heterocyclic Lewis bases. Eight mononuclear complexes of the general formula $[\text{Ni}(\text{sal4-Phtsc})\cdot\text{D}]$ and one dinuclear $\{[\text{Ni}(\text{sal4-Phtsc})]_2\cdot\text{D}\}\cdot 2\text{DMSO}$ complex were synthesized.

The structures of complexes where D is an imidazole (**1**), 4,4'-bipyridine (**5**), morpholine (**7**) and thiomorpholine (**8**) are the same in the solid state and in $[\text{D}_6]\text{DMSO}$, while complexes **2** (2-methylimidazole), **3** (pyridine), **4** (4-aminopyridine), **6** (4-methylpyridine) and **9** (2-aminophenol) decompose very fast, producing a $[\text{Ni}(\text{sal-4-phtsc})(\text{DMSO})]$ complex. All these results are in accordance with theoretical calculations of the standard Gibbs energies of binding, except in the case of complex **4** where interchange of 4-aminopyridine with DMSO is mostly controlled by kinetics.^[21] The experimental structural and spectroscopic data are in good agreement with the calculated standard Gibbs energies of binding. A linear correlation model between the experimentally measured distances and the calculated standard Gibbs energies of binding for all ligands (except for 4,4'-bipyridine) gives the R^2 value of 0.97 confirming the validity of the theoretical methods. All the results showed the preferred binding affinity toward the N-donor atom compared to the O- or S-donor atoms and could explain the easy substitution of the S-bonded $\text{H}_2\text{sal4-Phtsc}$ in the parent $[\text{Ni}(\text{sal4-Phtsc})(\text{H}_2\text{sal4-Phtsc})]\cdot\text{CH}_3\text{OH}$ complex.

The stability of complexes is strongly connected with nucleophilicity of the N-donor atom, but also with the polarity of the solvents since stability of all complexes is lower with the increase of the solvent dielectric constant. A comparison of the calculated standard Gibbs energies of binding with the single-crystal X-ray data leads to the conclusion that complexes **1**, **3**, **4** and **6** are thermodynamically more stable than the others and that the cyclic dimerization obtained either by N–H \cdots N (in **1**) or by the N–H \cdots S (**3**, **4** and **6**) intermolecular hydrogen bonds contributes to the additional stabilization in the context of the crystal packing framework. The results of the presented structural data and the spectroscopic and quantum mechanical analysis show these types of complexes as possible models for the explanation of catalytic and biological activity of Ni^{II} because of the labile fourth coordination site with the S-, O- or N-donor ligand.

Experimental Section

Materials: Salicylaldehyde, 4-phenylthiosemicarbazide, $\text{Ni}(\text{OAc})_2\cdot 4\text{H}_2\text{O}$, imidazole, 2-methylimidazole, pyridine, 4-aminopyridine, 4,4'-bipyridine, γ -picoline, morpholine, thiomorpholine and 2-aminophenol were commercially available and used as received. The ligand H_2L (salicylaldehyde 4-phenylthiosemicarbazone) and complex $[\text{Ni}(\text{sal4-Phtsc})(\text{H}_2\text{sal4-Phtsc})]\cdot\text{CH}_3\text{OH}$ were prepared according to the literature procedure.^[16] The methanol was of reagent grade and used as received. IR spectra for the parent complex and complexes **1–9** can be found in the Supporting Information [Figure S1(a)–Figure S1(j)].

Synthesis of the Complexes

General Method: The methanol solution of the N-donor (imidazole, 2-methylimidazole, pyridine, 4-aminopyridine, 4,4'-bipyridine, γ -

picoline, 2-aminophenol), N/O (morpholine) or N/S ligand (thiomorpholine) (2.5 mol) was added to the suspension of $[\text{Ni}(\text{sal4-Phtsc})(\text{H}_2\text{sal4-Phtsc})]\cdot\text{CH}_3\text{OH}$ (1 mol) and heated until the clear reddish solution (without precipitate) was obtained. After a few days, the crystals of **1–4** and **6–9** were filtered off, washed with a small amount of cold alcohol and dried. In the case of **5**, the reaction was instantaneous and the precipitate was present at all times. The crystals of **5** were obtained by recrystallization from the mixture of DMSO and acetone.

1: Yield 100.2 mg (63.27%). $\text{C}_{17}\text{H}_{15}\text{N}_5\text{NiOS}$ (396.09): calcd. C 51.55, H 3.82, N 17.68, Ni 14.82, S 8.09; found C 51.12, H 3.65, N 17.30, Ni 14.41, S 7.80. IR (KBr): $\tilde{\nu} = 3179 \nu_{(\text{NH})}$; 3127 $\nu_{(\text{NHimidazole})}$; 1601, 1583 $\nu_{(\text{C=N})}$; 1556 $\nu_{(\text{C=Nimidazole})}$; 1152 $\nu_{(\text{C=Ophen})}$; 658 $\nu_{(\text{CS})}$ cm^{-1} .

2: Yield 127.2 mg (77.79%). $\text{C}_{18}\text{H}_{18}\text{N}_5\text{NiOS}$ (410.11): calcd. C 52.71, H 4.18, N 17.07, Ni 14.31, S 7.82; found C 52.38, H 3.82, N 16.58, Ni 14.19, S 7.55. IR (KBr): $\tilde{\nu} = 3324 \nu_{(\text{NH})}$, $\nu_{(\text{OH})}$; 1603, 1587 $\nu_{(\text{C=N})}$; 1555 $\nu_{(\text{C=Nimidazole})}$; 1148 $\nu_{(\text{C=Ophen})}$; 689 $\nu_{(\text{CS})}$ cm^{-1} .

3: Yield 127.2 mg (77.79%). $\text{C}_{19}\text{H}_{16}\text{N}_4\text{NiOS}$ (407.05): calcd. C 56.05, H 3.96, N 13.76, Ni 14.42, S 7.87; found C 55.87, H 3.56, N 13.31, Ni 14.21, S 7.53. IR (KBr): $\tilde{\nu} = 3249 \nu_{(\text{OH})}$, $\nu_{(\text{NH})}$; 1606, 1587 $\nu_{(\text{C=N})}$; 1555 $\nu_{(\text{C=Npy})}$; 1143 $\nu_{(\text{C=Ophen})}$; 668 $\nu_{(\text{CS})}$ cm^{-1} .

4: Yield 132.6 mg (78.21%). $\text{C}_{19}\text{H}_{17}\text{N}_5\text{NiOS}$ (422.13): calcd. C 54.06, H 4.06, N 16.59, Ni 13.90, S 7.59; found C 53.70, H 3.63, N 16.32, Ni 13.73, S 7.09. IR (KBr): $\tilde{\nu} = 3348 \nu_{(\text{OH})}$, $\nu_{(\text{NH})}$; 3300, 3179 $\nu_{(\text{NHpy})}$; 1600, 1593 $\nu_{(\text{C=N})}$; 1554 $\nu_{(\text{C=Npy})}$; 1162 $\nu_{(\text{C=Ophen})}$; 668 $\nu_{(\text{CS})}$ cm^{-1} .

5: Yield 139.4 mg (85.41%). $\text{C}_{42}\text{H}_{42}\text{N}_8\text{Ni}_2\text{O}_4\text{S}_4$ (968.50): calcd. C 52.09, H 4.37, N 11.56, Ni 12.12, S 13.24; found C 52.22, H 4.38, N 11.65, Ni 12.01, S 13.31. IR (KBr): $\tilde{\nu} = 3346 \nu_{(\text{OH})}$, $\nu_{(\text{NH})}$; 1601, 1581 $\nu_{(\text{C=N})}$; 1559 $\nu_{(\text{C=Nbpy})}$; 1148 $\nu_{(\text{C=Ophen})}$; 668 $\nu_{(\text{CS})}$ cm^{-1} .

6: Yield 134.3 mg (79.39%). $\text{C}_{20}\text{H}_{18}\text{N}_4\text{NiOS}$ (421.14): calcd. C 57.04, H 4.31, N 13.30, Ni 13.94, S 7.61; found C 56.87, H 4.08, N 12.95, Ni 13.70, S 7.10. IR (KBr): $\tilde{\nu} = 3349 \nu_{(\text{OH})}$, $\nu_{(\text{NH})}$; 1606, 1587 $\nu_{(\text{C=N})}$; 1554 $\nu_{(\text{C=Npic})}$; 1150 $\nu_{(\text{C=Ophen})}$; 668 $\nu_{(\text{CS})}$ cm^{-1} .

7: Yield 146.37 mg (87.75%). $\text{C}_{18}\text{H}_{20}\text{N}_4\text{NiO}_2\text{S}$ (415.13): calcd. C 52.08, H 4.85, N 13.50, Ni 14.14, S 7.72; found C 51.55, H 4.48, N 12.89, Ni 14.05, S 7.61. IR (KBr): $\tilde{\nu} = 3332 \nu_{(\text{OH})}$, $\nu_{(\text{NH})}$; 3214 $\nu_{(\text{NHmorph})}$; 1602, 1586 $\nu_{(\text{C=N})}$; 1112 $\nu_{(\text{C=Nmorph})}$; 1148 $\nu_{(\text{C=Ophen})}$; 692 $\nu_{(\text{CS})}$ cm^{-1} .

8: Yield 146.06 mg (84.30%). $\text{C}_{18}\text{H}_{20}\text{N}_4\text{NiOS}_2$ (431.20): calcd. C 50.14, H 4.67, N 12.99, Ni 13.61, S 14.87; found C 49.92, H 4.19, N 12.46, Ni 13.43, S 14.67. IR (KBr): $\tilde{\nu} = 3392 \nu_{(\text{OH})}$, $\nu_{(\text{NH})}$; 3180 $\nu_{(\text{Nthiomorph})}$; 1600, 1584 $\nu_{(\text{C=N})}$; 1114 $\nu_{(\text{C=Nthiomorph})}$; 1150 $\nu_{(\text{C=Ophen})}$; 688 $\nu_{(\text{CS})}$ cm^{-1} .

9: Yield 127.2 mg (77.79%). $\text{C}_{20}\text{H}_{18}\text{N}_4\text{NiO}_2\text{S}$ (437.14): calcd. C 54.95, H 4.15, N 12.82, Ni 13.43, S 7.33; found C 54.78, H 3.83, N 12.36, Ni 13.32, S 7.18. IR (KBr): $\tilde{\nu} = 3316 \nu_{(\text{OH})}$, $\nu_{(\text{NH})}$; 1604, 1586 $\nu_{(\text{C=N})}$; 1212 $\nu_{(\text{C=Naminophenol})}$; 1150 $\nu_{(\text{C=Ophen})}$; 690 $\nu_{(\text{CS})}$ cm^{-1} .

Methods: Elemental analyses were carried out with a Perkin–Elmer Series II 2400 CHNS/O analyser. Infrared spectra were recorded with a Perkin–Elmer Spectrum RXI FTIR spectrometer from samples dispersed in KBr pellets (4000–400 cm^{-1} range).

The ^1H NMR spectra were recorded at 25 °C (and at 90 °C for complexes **8** and **9**) in $[\text{D}_6]\text{DMSO}$ with a Bruker AV-600 spectrometer operating at 600.13 MHz. Variable-temperature ^1H NMR experiments were carried out at 25, 0, –25 and –50 °C in $[\text{D}_7]\text{DMF}$ on the same instruments. The signal assignment (Table S1) was based on the chemical shifts and spin-spin couplings, two dimen-

sional experiments and quantum chemical calculations of the chemical shifts. The ^1H - ^1H COSY spectra were obtained at 25 °C in the magnitude mode with 2048 points in the F2 dimension and 512 increments in the F1 dimension.

X-ray Diffraction Experiments: The selected crystallographic and refinement data for the structures **1** and **3–8** (Figure 1) obtained by the single-crystal X-ray diffraction experiments are summarized in Table S2. The selected geometries including valence bonds and angles, hydrogen bonds and interaction geometries are given in Table 1 and Table S3. The data collection has been performed by applying the CrysAlis Software system,^[23] Versions 1.171.33.66 or 1.171.34.40 on the Oxford Xcalibur diffractometer supplied by CCD detector and graphite-monocromated Mo- K_α radiation ($\lambda = 0.71703 \text{ \AA}$) (structures **1** and **4**), Oxford Xcalibur Nova diffractometer and with graphite-monocromated Cu- K_α radiation ($\lambda = 1.54184 \text{ \AA}$) (structures **3**, **5**, **6**) and Oxford Xcalibur Gemini diffractometer equipped with Sapphire CCD detector and graphite-monocromated Cu- K_α radiation ($\lambda = 1.5418 \text{ \AA}$) (structures **7** and **8**). The data were collected at 296(2) K (structures **3**, **5–8**) or 120(2) K (structure **4**) all by using ω -scan. Programs CrysAlis CCD and CrysAlis RED^[23] were employed for cell refinement and data reduction in all cases. The Lorentz-polarization effect was corrected and the diffraction data have been scaled for the absorption effects by the multi-scanning method. The structures were solved by direct methods and refined on F^2 by weighted full-matrix least-squares. Programs SHELXS97 and SHELXL97^[24] integrated in the WinGX^[25] v. 1.80.05 software system were used to solve and refine structures. All non-hydrogen atoms were refined with the anisotropic displacement parameters. The hydrogen atoms belonging to the stereochemically different carbon atoms were placed in geometrically idealized positions with assigned isotropic displacement parameters and they were constrained to ride on their parent atoms by using the appropriate SHELXL97 HFIX instructions. The hydrogen atoms belonging to the nitrogen atom of the $-\text{NHPh}$ fragment in all structures were found as a small electron density in the difference Fourier map and the N–H distance has been restrained to the target value of 0.86(2) \AA by a SHELXL97 DFIX instruction (the DFIX instruction was not applied for **1** and **4**, already freely refined) (or by constrained instruction HFIX 43 for the N23 atom in complex **8**) with assigned isotropic displacement parameters constrained to 1.2 times the equivalent isotropic displacement parameters of the nitrogen atom that the hydrogen binds to. The hydrogen atoms of the amino group at the N5 atom in **4** were refined without DFIX restraint. The target N–H bond length value of 0.91 \AA for the morpholine ligand in **7** has been generated by the HFIX 13 instruction with $U_{\text{iso}}(\text{H}) = -1.2U_{\text{eq}}(\text{N})$ and thiomorpholine in **8** has been restrained to 0.89(2) \AA with $U_{\text{iso}}(\text{H}) = -1.2U_{\text{eq}}(\text{N})$ at N14 and N24.

The bipyridine derivative **5** crystallizes with the two DMSO molecules as solvent of crystallization. One of the molecules demonstrates positional disorder of the sulfur atom, which has been refined using the FVAR second variable SHELXL97 instruction to allow free refinement of particular occupancies for two sulfur atom positions. Then partial occupancies were rounded with the values of 58:42 to simplify the formula at the end of the refinement procedure. The molecular geometry calculations especially those including hydrogen bonding and non-covalent interactions were performed using the programs PLATON^[26] and PARST95^[27] integrated in the WinGX software system.^[25] The program Mercury^[28] was used for the molecular visualization. All molecular structure overviews and packing diagrams are rendered by the Pov-Ray program.^[29] An analogous atom-labelling scheme has been applied for all atoms in the structures **1** and **3–8** for reasons of comparison.

Quantum Chemical Calculations: Quantum chemical calculations were performed using the Gaussian 09 program package.^[29] The geometry optimization for the ground and the transition states were performed at the B3LYP/6-311++G(d,p) level of theory.^[30,31] For all optimized structures the harmonic frequencies were calculated to insure that obtained geometries correspond to the local minimum (or maximum) on the potential energy surface. The Gibbs energies were calculated at $T = 298.15 \text{ K}$ and $p = 101.325 \text{ kPa}$ and the data are given in Table 2. The solvation effects were incorporated in the calculations using the reformulation of the polarizable continuum model (PCM),^[32,33] known as integral equation formalism (IEFPCM) of Tomasi and coworkers.^[34–37]

Supporting Information (see footnote on the first page of this article): The supplementary materials contain: IR spectra for the parent complex and complexes **1–9**, superimposition of the experimental XRPD patterns for complexes **1–9**, the Mercury Pov-Ray overviews with full atom-labelling scheme for complexes **3**, **4** and **6–8**, superimposition of complex **3** and a previously published polymorph as well as overlaying of their calculated powder patterns from the single-crystal X-ray data, the overlaying diagram of the two crystallographically independent molecules in **8**, the extended packing diagrams for the complexes **3**, **4**, **5**, **6**, **7** and **8**, ^1H NMR spectra of complex **9**, ^1H NMR spectroscopic data in DMSO solution for the complexes **1–9** with corresponding atom numbering of the ligands used in the assignment of NMR resonances (Scheme S1), the table of crystallographic data for complexes **1** and **3–8**, the table of hydrogen bonding and contact geometries, the table of the selected calculated dihedral angles for the thiosemicarbazonato ligand and the table of the selected torsion angles for the thiosemicarbazonato ligand.

CCDC-887907 (for **1**), -887908 (for **3**), -887909 (for **4**), -887910 (for **5**), -887911 (for **6**), -887912 (for **7**), -887913 (for **8**) contain the supplementary crystallographic data for this paper. These data can be obtained free of charge from The Cambridge Crystallographic Data Centre via www.ccdc.cam.ac.uk/data_request/cif.

Acknowledgments

This research was supported by the Ministry of Science, Education and Sports of the Republic of Croatia (grant numbers 119-1191342-1082, 119-1191342-2959 and 098-0982915-2950).

- [1] S. W. Ragsdale, *J. Inorg. Biochem.* **2007**, *101*, 1657–1666.
- [2] S. W. Ragsdale, *J. Biol. Chem.* **2009**, *284*, 18571–18575.
- [3] M. A. Halcrow, G. Christou, *Chem. Rev.* **1994**, *94*, 2421–2481.
- [4] V. Mathrubootham, J. Thomas, R. Staples, J. McCracken, J. Shearer, E. J. Hegg, *Inorg. Chem.* **2010**, *49*, 5393–5406.
- [5] S. W. Ragsdale, M. Kumar, *Chem. Rev.* **1996**, *96*, 2515–2539.
- [6] F. Bisceglie, M. Baldini, M. Belicchi-Ferrari, *Eur. J. Med. Chem.* **2007**, *42*, 627–634.
- [7] A. Buschini, S. Pinelli, C. Pellacani, *J. Inorg. Biochem.* **2009**, *103*, 666–677.
- [8] N. C. Kasuga, K. Sekino, C. Koumo, N. Shimada, M. Ishikawa, K. Nomiyama, *J. Inorg. Biochem.* **2001**, *84*, 55–65.
- [9] a) P. Novak, K. Pićuljan, T. Hrenar, T. Biljan, Z. Meić, *J. Mol. Struct.* **2009**, *919*, 66; b) V. Vrdoljak, M. Cindrić, D. Milić, D. Matković-Čalogović, P. Novak, B. Kamenar, *Polyhedron* **2005**, *24*, 1717–1726; c) M. Cindrić, V. Vrdoljak, N. Strukan, B. Kamenar, *Polyhedron* **2005**, *24*, 369–376; d) M. Cindrić, M. Rubčić, I. Đilović, G. Giester, B. Kamenar, *Croat. Chem. Acta* **2007**, *80*, 583–590; e) I. Đilović, M. Rubčić, V. Vrdoljak, S. Kraljević Pavelić, M. Kralj, I. Piantanida, M. Cindrić, *Bioorg. Med. Chem.* **2008**, *16*, 5189–5198; f) M. Rubčić, D. Milić, G.

- Horvat, I. Đilović, N. Galić, V. Tomišić, M. Cindrić, *Dalton Trans.* **2009**, *44*, 9914–9923; g) V. Vrdoljak, I. Đilović, M. Rubčić, S. Kraljević Pavelić, M. Kralj, D. Matković-Čalogović, I. Piantanida, A. Rožman, M. Cindrić, *Eur. J. Med. Chem.* **2010**, *45*, 38–48; h) M. Rubčić, D. Milić, G. Pavlović, M. Cindrić, *Cryst. Growth Des.* **2011**, *11*, 5227–5240.
- [10] a) E. Labisbal, K. D. Haslow, A. Sousa-Pedrares, J. Valdes-Martinez, S. Hernandez-Ortega, D. X. West, *Polyhedron* **2003**, *22*, 2831–2837; b) A. Castineiras, M. Gil, E. Bermejo, D. X. West, *Polyhedron* **2001**, *20*, 449–454; c) G. E. de Sousa, L. C. C. Manso, E. S. Lang, C. C. Gatto, B. Mahie, *J. Mol. Struct.* **2007**, *826*, 185–191.
- [11] T. S. Lobana, R. Sharma, G. Bawa, S. Khanna, *Coord. Chem. Rev.* **2009**, *253*, 977–1055.
- [12] a) N. C. Kasuga, K. Sekino, C. Koumo, N. Shimada, M. Ishikawa, K. Nomiyama, *J. Inorg. Biochem.* **2001**, *84*, 55–65; b) N. C. Kasuga, K. Sekino, M. Ishikawa, A. Honda, M. Yokoyama, S. Nakano, N. Shimada, C. Loumo, K. Nomiyama, *J. Inorg. Biochem.* **2003**, *96*, 298–310.
- [13] a) P. Dapporto, G. De Munno, A. G. Tomlison, *J. Chem. Res.* **1984**, *40*, 501–502; b) S. V. Kolotilov, O. Cador, S. Golhen, O. Shvets, V. G. Ilyin, V. V. Pavlischuk, L. Ouahab, *Inorg. Chim. Acta* **2007**, *360*, 1883–1889; c) E. Gyepes, F. Pavelcik, A. Beno, *Collect. Czech. Chem. Commun.* **1981**, *46*, 975–981; d) E. Gyepes, T. Glowiak, *Acta Crystallogr., Sect. C* **1989**, *45*, 391–392; e) M. Soriano-García, R. A. Toscano, J. Valdés-Martínez, J. M. Fernández, *Acta Crystallogr., Sect. C* **1985**, *41*, 498–500; f) R. Prabhakaran, R. Karvembu, T. Hashimoto, K. Shimizu, K. Natarajan, *Inorg. Chim. Acta* **2005**, *358*, 2093–2096; g) B. F. Hoskins, R. Robson, H. Schaap, *Inorg. Nucl. Chem. Lett.* **1972**, *8*, 21–25; h) Z. Lu, C. White, A. L. Rheingold, R. H. Crabtree, *Inorg. Chem.* **1993**, *32*, 3991–3994; i) L. Latheef, M. R. P. Kurup, *Polyhedron* **2008**, *27*, 35–43; j) B. Ülküseven, T. Bal Demirci, M. Akkurt, S. P. Yalcin, O. Buykgungor, *Polyhedron* **2008**, *27*, 3646–3652; k) Z.-Y. Cao, Z.-P. Deng, S. Gao, *Acta Crystallogr., Sect. E* **2007**, *63*, m1961–m1962; l) S. Guveli, T. Bal Demirci, N. Ozdemir, N. Ülküseven, *Transition Met. Chem.* **2009**, *34*, 383–388; m) H. B. Shawish, K. W. Tan, M. J. Maah, S. W. Ng, *Acta Crystallogr., Sect. E* **2010**, *66*, m1074; n) T. S. Lobana, P. Kumari, G. Hundal, R. J. Butcher, *Polyhedron* **2010**, *29*, 1130–1136; o) H. B. Shawish, M. J. Maah, S. W. Ng, *Acta Crystallogr., Sect. E* **2010**, *66*, m1366; p) V. V. Bon, S. I. Orysyk, V. I. Pekhnyo, S. V. Volkov, *J. Mol. Struct.* **2010**, *984*, 15–22; q) R. Prabhakaran, R. Sivasamy, J. Angayarkanni, R. Huang, P. Kalaivani, R. Karvembu, F. Dallemer, K. Natarajan, *Inorg. Chim. Acta* **2011**, *374*, 647–653.
- [14] a) J. Y. Gao, Z. Liu, Y. Wang, *Acta Crystallogr., Sect. E* **2009**, *65*, m523–m524; b) G. Schulte, X. L. Luo, R. H. Crabtree, M. Zimmer, *Angew. Chem.* **1991**, *103*, 205; *Angew. Chem. Int. Ed. Engl.* **1991**, *30*, 193–194; c) P. X. García-Reynaldos, S. Hernández-Ortega, R. A. Toscano, J. Valdés Martínez, *Supramol. Chem.* **2007**, *19*, 613–619; d) Y. T. Wang, H. L. Li, J. G. Wang, *Z. Kristallogr. New Cryst. Struct.* **2010**, *225*, 79; e) X. H. Qiu, H. Y. Wu, *Acta Crystallogr., Sect. E* **2004**, *60*, m1151–m1152; f) K. K. Du, S. X. Liu, *J. Mol. Struct.* **2008**, *874*, 138–144; g) L. Latheef, E. B. Seená, M. R. P. Kurup, *Polyhedron* **2009**, *28*, 2515–2518; h) A. Berkessel, G. Hermann, O.-T. Rauch, M. Buchner, A. Jacobi, G. Huttner, *Chem. Ber.* **1996**, *129*, 1421–1423; i) Y. D. Kurt, B. Ülküseven, *J. Coord. Chem.* **2010**, *63*, 828–836.
- [15] a) D. Kovala, J. R. Miller, N. Kurkomelis, S. K. Hadikakon, M. A. Demetris, *Polyhedron* **1999**, *18*, 1005–1013; b) Y. Yu, D. S. Kalinowski, Z. Kovacević, A. R. Sifakas, P. J. Jansson, C. Stefani, D. B. Lovejoy, P. C. Sharpe, P. V. Bernhardt, D. R. Richardson, *J. Med. Chem.* **2009**, *52*, 5271–5294; c) Y. Li, Z. Y. Yang, J. C. Wu, *Eur. J. Med. Chem.* **2010**, *45*, 5692–5701; d) M. B. Ferrari, F. Bisceglie, G. Pelosi, P. Tarasconi, R. Albertini, A. Bonati, P. Lunghi, S. Pinelli, *J. Inorg. Biochem.* **2002**, *90*, 113–126; e) M. B. Ferrari, F. Bisceglie, G. Pelosi, P. Tarasconi, R. Albertini, P. P. Dall’Aglio, S. Pinelli, A. Bergamo, G. Sava, *J. Inorg. Biochem.* **2004**, *98*, 301–312; f) M. A. Ali, A. H. Mirza, A. M. S. Hossain, M. Nazimuddin, *Polyhedron* **2001**, *20*, 1045–1052; g) M. Joseph, M. Kuriakose, M. R. P. Kurup, E. Suresh, A. Kishore, S. G. Bhat, *Polyhedron* **2006**, *25*, 61–70.
- [16] M. Cindrić, M. Uzelac, D. Cinčić, I. Halasz, G. Pavlović, T. Hrenar, M. Čurić, D. Kovačević, *CrystEngComm* **2012**, *14*, 3039–3045.
- [17] C. R. Kowol, R. Trondl, P. Heffeter, V. B. Arion, M. A. Jakupc, A. Roller, M. Galanski, W. Berger, B. K. Keppler, *J. Med. Chem.* **2009**, *52*, 5032–5043.
- [18] a) S. K. Jain, B. S. Garg, Y. K. Bhoon, *Spectrochim. Acta Part A* **1986**, *42*, 959–968; b) G. Pelosi, *Open Crystallogr. J.* **2010**, *3*, 16–28; c) H. Beraldo, D. Gambino, *Mini-Rev. Med. Chem.* **2004**, *4*, 31–39.
- [19] E. B. Seená, P. M. R. Kurup, E. Suresh, *J. Chem. Crystallogr.* **2008**, *38*, 93–96.
- [20] a) F. A. Cotton, R. Francis, *J. Am. Chem. Soc.* **1960**, *82*, 2986–2991; b) F. A. Cotton, R. Francis, W. D. Horrocks Jr., *J. Am. Chem. Soc.* **1960**, *82*, 1534–1536.
- [21] a) T. L. Ho, *Chem. Rev.* **1975**, *75*, 1–20; b) R. G. Pearson, *J. Am. Chem. Soc.* **1963**, *85*, 3533.
- [22] a) M. Cindrić, V. Vrdoljak, N. Strukan, B. Kamenar, *Polyhedron* **2005**, *24*, 369–376; b) V. Vrdoljak, I. Đilović, M. Rubčić, S. Kraljević Pavelić, M. Kralj, D. Matković-Čalogović, I. Piantanida, P. Novak, A. Rožman, M. Cindrić, *Eur. J. Med. Chem.* **2010**, *45*, 38–48.
- [23] Oxford Diffraction Ltd., *Xcalibur CCD system*, CrysAlis Software system, version 1.171.33.66 Abingdon, Oxfordshire, England, **2010**.
- [24] G. M. Sheldrick, *Acta Crystallogr., Sect. A* **2008**, *64*, 112–122.
- [25] L. J. Farrugia, *J. Appl. Crystallogr.* **1999**, *32*, 837–838.
- [26] A. Spek, *J. Appl. Crystallogr.* **2003**, *36*, 7–13.
- [27] M. Nardelli, *J. Appl. Crystallogr.* **1995**, *28*, 659.
- [28] M. J. Frisch, G. W. Trucks, H. B. Schlegel, G. E. Scuseria, M. A. Robb, J. R. Cheeseman, G. Scalmani, V. Barone, B. Mennucci, G. A. Petersson, H. Nakatsuji, M. Caricato, X. Li, H. P. Hratchian, A. F. Izmaylov, J. Bloino, G. Zheng, J. L. Sonnenberg, M. Hada, M. Ehara, K. Toyota, R. Fukuda, J. Hasegawa, M. Ishida, T. Nakajima, Y. Honda, O. Kitao, H. Nakai, T. Vreven, J. A. Montgomery Jr, J. E. Peralta, F. Ogliaro, M. Bearpark, J. J. Heyd, E. Brothers, K. N. Kudin, V. N. Staroverov, R. Kobayashi, J. Normand, K. Raghavachari, A. Rendell, J. C. Burant, S. S. Iyengar, J. Tomasi, M. Cossi, N. Rega, J. M. Millam, M. Klene, J. E. Knox, J. B. Cross, V. Bakken, C. Adamo, J. Jaramillo, R. Gomperts, R. E. Stratmann, O. Yazyev, A. J. Austin, R. Cammi, C. Pomelli, J. W. Ochterski, R. L. Martin, K. Morokuma, V. G. Zakrzewski, G. A. Voth, P. Salvador, J. J. Dannenberg, S. Dapprich, A. D. Daniels, O. Farkas, J. B. Foresman, J. V. Ortiz, J. Cioslowski, D. J. Fox, *Gaussian 09*, rev. A.02, Gaussian, Inc., Wallingford CT, **2009**.
- [29] www.povray.org.
- [30] A. D. Becke, *J. Chem. Phys.* **1993**, *98*, 5648–5653.
- [31] C. Lee, W. Yang, R. G. Parr, *Phys. Rev. B* **1988**, *37*, 785–789.
- [32] S. Miertuš, E. Scrocco, J. Tomasi, *Chem. Phys.* **1981**, *55*, 117–129.
- [33] J. Tomasi, M. Persico, *Chem. Rev.* **1994**, *94*, 2027–2094.
- [34] E. Cancès, B. Mennucci, *J. Math. Chem.* **1998**, *23*, 309–326.
- [35] A. Murugkar, S. Padhye, S. Guha-Roy, U. Wagh, *Inorg. Chem. Commun.* **1999**, *2*, 545–548.
- [36] S. K. Jain, B. S. Garg, Y. K. Bhoon, *Spectrochim. Acta* **1986**, *42A*, 959–968.
- [37] M. Rubčić, I. Đilović, M. Cindrić, D. Matković-Čalogović, *Acta Crystallogr., Sect. C* **2008**, *64*, o570–o573.

Received: September 11, 2012

Published Online: December 10, 2012